

1-15-1983

Observation of nonhexagonal superlattices in high-stage cesium intercalated graphite

D. M. Hwang

N. W. Parker

Mark Utlaut

University of Portland, utlaut@up.edu

A. V. Crewe

Follow this and additional works at: http://pilotscholars.up.edu/phy_facpubs

 Part of the [Plasma and Beam Physics Commons](#)

Citation: Pilot Scholars Version (Modified MLA Style)

Hwang, D. M.; Parker, N. W.; Utlaut, Mark; and Crewe, A. V., "Observation of nonhexagonal superlattices in high-stage cesium intercalated graphite" (1983). *Physics Faculty Publications and Presentations*. 38.

http://pilotscholars.up.edu/phy_facpubs/38

This Journal Article is brought to you for free and open access by the Physics at Pilot Scholars. It has been accepted for inclusion in Physics Faculty Publications and Presentations by an authorized administrator of Pilot Scholars. For more information, please contact library@up.edu.

Observation of nonhexagonal superlattices in high-stage cesium intercalated graphite

D. M. Hwang

*Department of Physics, University of Illinois at Chicago, Chicago, Illinois 60680*N. W. Parker,* M. Utlaut,[†] and A. V. Crewe*Enrico Fermi Institute, University of Chicago, Chicago, Illinois 60637*

(Received 6 August 1982)

Using a scanning transmission electron microscope with an electron beam size of $\sim 800 \text{ \AA}$, we have found that unsaturated cesium intercalated graphite at $98 \pm 2 \text{ K}$ exhibits multiple structural phases with a typical domain size of $\sim 1 \mu\text{m}$. Electron diffraction patterns from individual structural islands were studied, and the $p(2 \times 2)$, $p(\sqrt{3} \times 2)$, and $p(\sqrt{3} \times \sqrt{13})$ in-plane superlattices were identified.

The in-plane structures of intercalated molecules or atoms in graphite intercalation compounds (GIC's) have been extensively studied for many years.¹ In several GIC's, the x-ray or electron diffraction patterns exhibit distinct diffraction spots, indicating that the intercalated layers are of ordered structures, but the patterns cannot be interpreted by simple in-plane structures.¹ It has been proposed^{1,2} that, in those GIC's, several structural phases may coexist even in well-staged samples. The traditional diffraction probe beam size is $\sim 1 \text{ mm}$ for x rays and $\sim 1 \mu\text{m}$ for electrons from conventional transmission electron microscopes. Several studies²⁻⁸ have suggested that the typical size of the structural islands is smaller than the size of their probe beams, and their observed patterns consist of diffractions from many domains of various structures.

The stage-1 heavy alkali-metal intercalated graphite compounds are among the few GIC's whose in-plane structures have been well established. However, their high-stage compounds exhibit many interesting structural phases which are not yet fully characterized.¹ Consider the high-stage Cs-graphite compound at liquid-nitrogen temperature as an example. An early x-ray study² suggested the coexistence of (2×2) , $(3 \times \sqrt{7})$, $(\sqrt{39} \times \sqrt{39})$, and $(\sqrt{7} \times \sqrt{7})$ superlattices. The $(3 \times \sqrt{7})$ and $(\sqrt{39} \times \sqrt{39})$ phases were "characterized by diffraction patterns having an abnormally large number of unobservable reflections."² A recent study^{3,4} proposed a structure of a modulated incommensurate triangular lattice orientationally locked to the graphite lattice in coexistence with the (2×2) commensurate phase. Electron diffraction studies^{5,6} with $\sim 1 \mu\text{m}$ beam size yield very complicated patterns. Unlike the cases of Rb-graphite⁷ and K-graphite,⁸ no detailed analysis has been published, but it is said⁶ that the structure is incommensurate.

A scanning transmission electron microscope (STEM) is used in this study to probe the diffraction

patterns from individual structural domains in high-stage Cs intercalated New York natural single-crystal graphite. The electron beam size on the sample was estimated to be $\sim 800 \text{ \AA}$. The STEM was operated with an electron energy of 18 keV and at $\sim 3 \times 10^{-10}$ Torr vacuum. The sample holder was in thermal contact with a liquid-nitrogen cold finger and was maintained at $98 \pm 2 \text{ K}$. Details of the experimental setup will be presented elsewhere.⁹

The sample suitable for STEM study must be only a few hundred \AA thick. Such a thin alkali-metal-graphite sample could be intercalated or deintercalated within a few seconds by the conventional two-temperature method. The sample is too thin to be characterized by the x-ray, neutron, or optical methods and is easily contaminated.

A vacuum sample transfer technique has been developed to handle air-sensitive GIC's.¹⁰ A "near-saturated" Cs-graphite sample was transferred at 10^{-9} Torr vacuum into the STEM and quenched to $98 \pm 2 \text{ K}$. A homogenous area of the sample of thickness $\sim 500 \text{ \AA}$ was found. The recorded electron diffraction pattern is similar to that shown in Fig. 1(b), indicating a (2×2) superlattice. This was the only pattern observed, and it remained unchanged for one week while the sample was maintained at $98 \pm 2 \text{ K}$ and 3×10^{-10} Torr vacuum. Therefore it is established that this near-saturated sample is essentially the stage-1 CsC₈.

The sample was then deintercalated at room temperature and 10^{-9} Torr vacuum for one week and cooled to $98 \pm 2 \text{ K}$ again. A typical bright-field image from this partially vacuum-desorbed sample is shown in Fig. 1(a). It clearly indicates the formation of islands with a characteristic dimension of $\sim 1 \mu\text{m}$. Several different types of diffraction patterns were observed, including the patterns shown in Figs. 1(b), 2(a), and 3(a), as well as patterns similar to Figs. 2(a) or 3(a), but rotated 60° clockwise or counterclockwise. By moving the electron beam a few μm

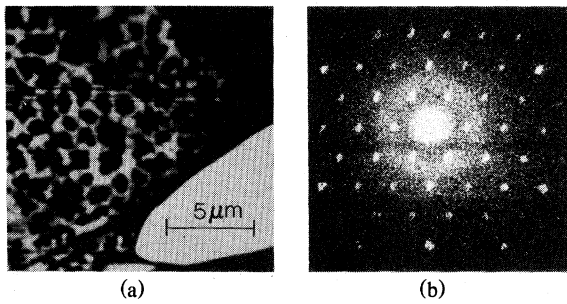


FIG. 1. Scanning transmission electron microscopic study of the unsaturated Cs-graphite sample at 98 ± 2 K. (a) The bright field image. The black area at the upper-right-hand corner is a part of the support grid. The white area at the lower-right-hand corner is a hole on the sample. (b) One of the diffraction patterns observed. This is the well-known (2×2) superlattice pattern.

across the sample, we were able to obtain any of the above patterns, or a superposition of two or three of them. At present, we are not able to correlate the observed pattern with the position in the direct image.

The pattern shown in Fig. 1(b) corresponds to the well-known (2×2) superlattice observed in stage-1 heavy alkali-metal graphite MC_8 ($M = K, Rb,$ and Cs). It is also established²⁻⁴ as one of the structural phases for high-stage Cs-graphite at liquid-nitrogen temperature.

The simple rectangular pattern shown in Fig. 2(a) can be matched by the $(\sqrt{3} \times 2)$ superlattice shown in Fig. 2(b). Figure 2(c) is the diffraction pattern constructed from Fig. 2(b). Three different orientations

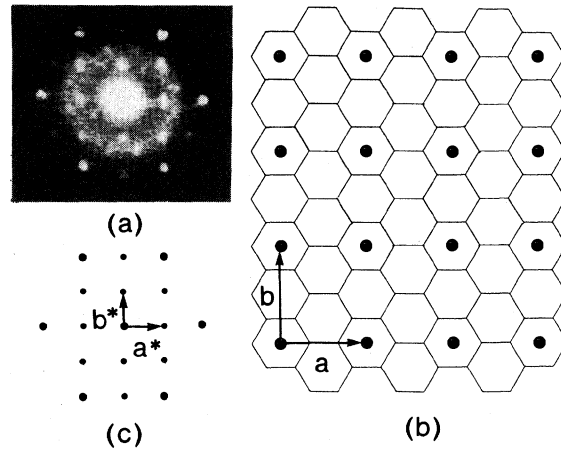


FIG. 2. (a) One of the diffraction patterns observed from the unsaturated Cs-graphite sample at 98 ± 2 K. (b) The $p(\sqrt{3} \times 2)$ in-plane superlattice on the graphite in-plane network. (c) The reciprocal lattice of (b). The large dots are due to the graphite lattice. The small dots result from the Cs superlattice.

of this pattern, corresponding to the three equivalent orientations of the $(\sqrt{3} \times 2)$ superlattice, have been observed. Actually, a set of faint spots can be observed in Fig. 2(a), which corresponds to the strong set rotated 60° counterclockwise.

The in-plane C:Cs ratio for the $p(\sqrt{3} \times 2)$ superlattice is 8:1. As can be seen in Fig. 2(b), moving every other column of Cs atoms in the $p(\sqrt{3} \times 2)$ lattice by a lattice constant up or down results in the

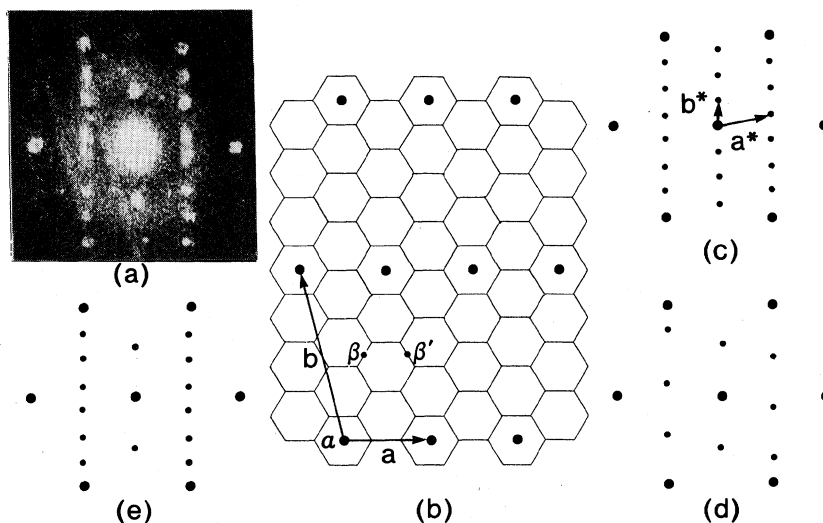


FIG. 3. (a) One of the diffraction patterns observed from the unsaturated Cs-graphite sample at 98 ± 2 K. (b) The $p(\sqrt{3} \times \sqrt{13})$ in-plane superlattice on the graphite in-plane network. (c) The reciprocal lattice of (b). (d) The diffraction pattern expected from a sample of a perfect $\alpha\beta$ stacking sequence. (e) The diffraction pattern expected from a mixture of $\alpha\beta$ and $\alpha\beta'$ stacking sequences.

$p(2 \times 2)$ lattice.

The superlattice associated with the pattern shown in Fig. 3(a) is less obvious. Since all diffraction spots fall on the vertical lines connecting the graphite spots, one of the translation vectors in real space must be $\sqrt{3}$. The diffraction spots are elongated along the vertical direction, indicating that the translation symmetry along this direction is poorly ordered. We find the pattern is best fitted by the $(\sqrt{3} \times \sqrt{13})$ superlattice. A simple $(\sqrt{3} \times \sqrt{13})$ superlattice is shown in Fig. 3(b), and its reciprocal lattice is shown in Fig. 3(c).

The $(\pm 1, k)$ spots in Fig. 3(c) are consistent with the observation. However, the $(0, \pm 1)$ and $(0, \pm 3)$ spots are missing from Fig. 3(a). This can be interpreted as being the result of the nearest-Cs-layer stacking correlation. In contrast to the $p(2 \times 2)$ superlattice, where an α layer can be followed by any one of the β , γ , and δ layers with equal probability, the $p(\sqrt{3} \times \sqrt{13})$ has preferred nearest-layer sites. If a Cs layer occupies the α sites as indicated in Fig. 3(b), then the next Cs layer has a tendency to locate near the centers of the α lattice, denoted as β or β' sites in Fig. 3(b). The Cs atoms should still be at the hexagon centers of the adjacent carbon layers and their exact positions depend on the graphite-layer stacking arrangement and the stage number. This kind of nearest-layer correlation always exists whether the long-range stacking sequence is ordered or not. For the sake of simplicity, we assume a perfect $\alpha\beta$ stacking sequence. The diffraction pattern becomes as shown in Fig. 3(d)—all (h, k) spots with odd $h + k$ disappear. A mixture of the $\alpha\beta$ and the $\alpha\beta'$ phases results in the diffraction pattern shown in Fig. 3(e) which is consistent with Fig. 3(a).

The in-plane C:Cs ratio is 14:1 for the $p(\sqrt{3} \times \sqrt{13})$ superlattice. It is interesting to note that a mixture of one-third $p(\sqrt{3} \times 2)$ with two-thirds $p(\sqrt{3} \times \sqrt{13})$ results in an in-plane C:Cs ratio of 12:1. A nonprimitive in-plane unit cell of $(\sqrt{3} \times 2)$ or $(\sqrt{3} \times \sqrt{13})$ will result in a too-high in-plane density.

Our unsaturated sample is prepared by vacuum desorption. Desorption under ultrahigh vacuum should be equivalent to deintercalation by the standard two-temperature method with the charge end kept near 0 K. Both should result in higher-stage compounds, possibly mixtures of several stages. A recent low-energy-electron diffraction (LEED) study showed that no surface adsorption layer results from vacuum desorption.¹¹ The x-ray⁴ and other studies¹ indicate that, for $n \geq 2$, the in-plane structures are not stage sensitive except some shifts in transition temperatures. Nevertheless, the structures we found are not consistent with the x-ray results.²⁻⁴ Similar conflicting observations exist between the x-ray and the electron diffraction studies for high-stage Rb-graphite⁷ and K-graphite.⁸ It seems that the in-plane structures for ultrathin GIC samples are different

from that of bulk samples. More progress in this field is needed to understand the structural differences of GIC's of various sizes, origins, and preparation conditions.

Both the nonhexagonal in-plane superlattice phases we observed, $p(\sqrt{3} \times 2)$ and $p(\sqrt{3} \times \sqrt{13})$, have an unusually small Cs nearest-neighbor distance of $\sqrt{3}a_0 = 4.27 \text{ \AA}$. This distance is less than that in the $p(2 \times 2)$ saturated phase ($2a_0 = 4.93 \text{ \AA}$), and that in Cs metal (5.24 \AA),¹² but still greater than the Cs ion diameter (3.34 \AA).¹² Our observations suggest that the Cs atoms in the less-saturated sample have a tendency to form chainlike structures. The nearest-neighbor distance is actually reduced with a reduction of the number of nearest neighbors. This phenomenon has not been predicted for graphite intercalation compounds. However, it is not new in two-dimensional physics. For example, a monolayer of gold atoms adsorbed on a silicon (111) surface between 400 and 700 °C exhibits a $(\sqrt{3} \times \sqrt{3})$ superlattice structure. While at a coverage between 0.2 to 0.5 monolayer, LEED study yields a starlike pattern which can be decomposed into three (1×5) superlattice patterns of equivalent orientations.¹³⁻¹⁵ Various models have been proposed to explain this result.^{13,14}

The in-plane structures for intercalation compounds are further complicated by the formation of staging and the interlayer correlation. The inter-intercalation-layer correlation certainly plays an essential role in the formation of in-plane structures, as evidenced by our observation that the same in-plane structure is preserved over more than 100 layers along the c axis. Models more elaborate than that for the surface adsorption system^{13,14} are required to describe the GIC structures.

A highly anisotropic superlattice will yield a diffraction pattern with spots closely packed on a few parallel lines. The superposition of these linelike patterns of various equivalent orientations results in a starlike pattern. Attempts to interpret such a pattern with a single superlattice will result in a very large unit cell and many missing diffraction spots.^{2,7} For example, the $C_{\nabla}X$ pattern of Kambe *et al.*⁷ has been interpreted as a superposition of $(\sqrt{12} \times \sqrt{12})$ and $(\sqrt{39} \times \sqrt{39})$ with many missing and extra diffraction spots. We found that the $C_{\nabla}X$ pattern can be matched by a superposition of $(\sqrt{3} \times \sqrt{7})$, $(\sqrt{3} \times 3)$, and $(\sqrt{3} \times 4)$, missing only one equivalent set of diffraction spots.

Finally, we point out that there may be other structural phases, especially those with diffuse scattering, which have escaped our observation. We are currently improving the performance of our STEM, and will then study the detailed temperature dependence of the island sizes, the intercalation density distribution, and the in-plane structures, as well as the correlation between various in-plane structures and their in-plane densities.

ACKNOWLEDGMENTS

We would like to thank Dr. M. Ohtsuki for many valuable discussions and technical assistance, and to Professor J. Curray for assistance in smoothing the English. This work is supported by the Research Board of the University of Illinois at Chicago, the National Science Foundation under Grant No. DMR NSF8014176, and the Materials Research Laboratories at the University of Chicago.

*Present address: Hughes Research Laboratory, Malibu, Cal. 90265.

†Present address: Varian Associates, Gloucester, Maine 01930.

¹For general background, consult the following two recent review articles: M. S. Dresselhaus and G. Dresselhaus, *Adv. Phys.* **30**, 139 (1981); S. A. Solin, *Adv. Chem. Phys.* **49**, 455 (1982).

²G. S. Parry, *Mater. Sci. Eng.* **31**, 99 (1977).

³R. Clarke, N. Caswell, S. A. Solin, and P. M. Horn, *Phys. Rev. Lett.* **43**, 2018 (1979).

⁴R. Clarke, N. Caswell, S. A. Solin, and P. M. Horn, *Physica (Utrecht)* **99B**, 457 (1980).

⁵D. D. L. Chung, G. Dresselhaus, and M. S. Dresselhaus, *Mater. Sci. Eng.* **31**, 107 (1977).

⁶M. S. Dresselhaus, N. Kambe, A. N. Berker, and G. Dresselhaus, *Synth. Met.* **2**, 121 (1980).

⁷N. Kambe, G. Dresselhaus, and M. S. Dresselhaus, *Phys. Rev. B* **21**, 3491 (1980).

⁸A. N. Berker, N. Kambe, G. Dresselhaus, and M. S. Dresselhaus, *Phys. Rev. Lett.* **45**, 1452 (1980).

⁹N. W. Parker, M. Utlaut, A. V. Crewe, and D. M. Hwang (unpublished).

¹⁰D. M. Hwang, M. Utlaut, M. Issacson, and S. A. Solin, *Phys. Rev. Lett.* **43**, 882 (1979).

¹¹N. J. Wu and A. Ignatiev, *Bull. Am. Phys. Soc.* **27**, 310 (1982).

¹²C. Kittel, *Introduction to Solid State Physics*, 5th ed. (Wiley, New York, 1976), pp. 32, 100.

¹³W. Haidinger and S. C. Barnes, *Surf. Sci.* **20**, 313 (1970).

¹⁴H. Lipson and K. W. Singer, *J. Phys. C* **7**, 12 (1974).

¹⁵G. Le Lay, G. Quentel, J. P. Faurie, and A. Masson, *Thin Solid Films* **35**, 289 (1976).

¹⁶D. M. Hwang, *Phys. Rev. B* (in press).

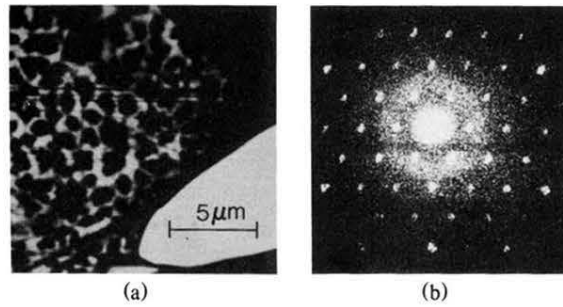


FIG. 1. Scanning transmission electron microscopic study of the unsaturated Cs-graphite sample at 98 ± 2 K. (a) The bright field image. The black area at the upper-right-hand corner is a part of the support grid. The white area at the lower-right-hand corner is a hole on the sample. (b) One of the diffraction patterns observed. This is the well-known (2×2) superlattice pattern.

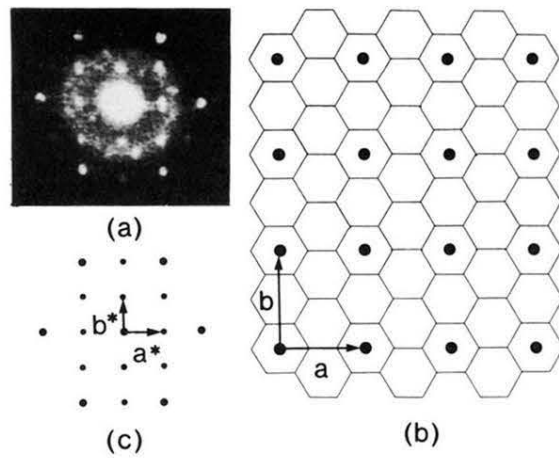


FIG. 2. (a) One of the diffraction patterns observed from the unsaturated Cs-graphite sample at 98 ± 2 K. (b) The $p(\sqrt{3} \times 2)$ in-plane superlattice on the graphite in-plane network. (c) The reciprocal lattice of (b). The large dots are due to the graphite lattice. The small dots result from the Cs superlattice.

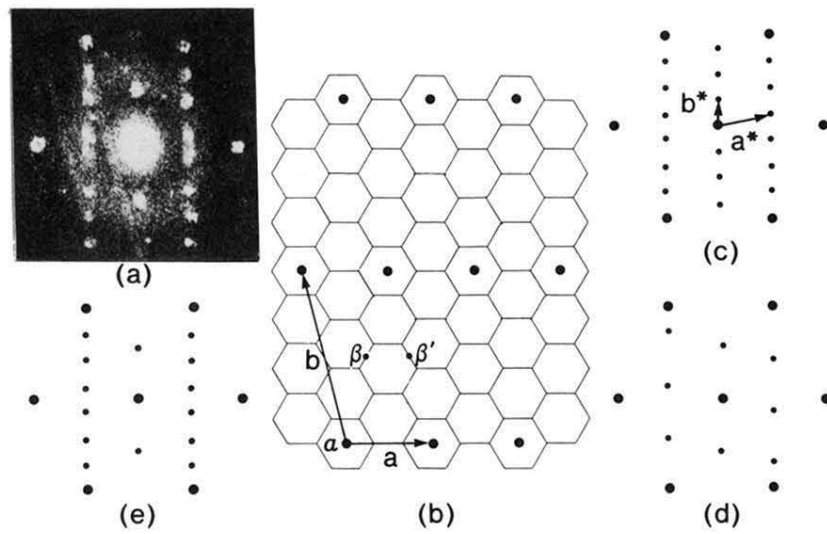


FIG. 3. (a) One of the diffraction patterns observed from the unsaturated Cs-graphite sample at 98 ± 2 K. (b) The $p(\sqrt{3} \times \sqrt{13})$ in-plane superlattice on the graphite in-plane network. (c) The reciprocal lattice of (b). (d) The diffraction pattern expected from a sample of a perfect $\alpha\beta$ stacking sequence. (e) The diffraction pattern expected from a mixture of $\alpha\beta$ and $\alpha\beta'$ stacking sequences.